ExSinGAN: Learning an Explainable Generative Model from a Single Image

Zi-Cheng Zhang[1] , **Cong-Ying Han**[1] , **Tian-De Guo**[1]

[1]University of Chinese Academy of Sciences

zhangzicheng19@mails.ucas.ac.cn, hancy, tdguo@ucas.ac.cn

Abstract

Generating images from a single sample, as a newly developing branch of image synthesis, has attracted extensive attention. In this paper, we formulate this problem as sampling from the conditional distribution of a single image, and propose a hierarchical framework that simplifies the learning of the intricate conditional distributions through the successive learning of the distributions about structure, semantics and texture, making the process of learning and generation comprehensible. On this basis, we design ExSinGAN composed of three cascaded GANs for learning an explainable generative model from a given image, where the cascaded GANs model the distributions about structure, semantics and texture successively. ExSinGAN is learned not only from the internal patches of the given image as the previous works did, but also from the external prior obtained by the GAN inversion technique. Benefiting from the appropriate combination of internal and external information, ExSinGAN has a more powerful capability of generation and competitive generalization ability for the image manipulation tasks compared with prior works.

1 Introduction

Recently, training single image generative models is getting more and more attention. Lately, [Shaham *et al.*, 2019] did groundbreaking work in this field, they proposed a pyramid of fully convolutional GANs [Goodfellow *et al.*, 2014] named SinGAN to learn the internal distribution of patches within the image. SinGAN has achieved great results in image synthesis, but it still has a lot of room for improvement, in which the synthesis mechanism is a weakness that needs to be improved. Imagining that how people draw a painting: if we want to create a painting based on a scene, firstly we need to have an approximate idea of the layout of our painting before the formal creation, then we draw the rough details of the objects in the scene step by step to make the painting look like the scene, and finally, we put fine details on the painting to make it delicate. It means that we should consider the structure, semantics, and fine details successively in order to generate images from a single image, thus the process

of generation is hierarchical and explainable. Although SinGAN is multi-stage, it is not hierarchical since each stage of the pyramid learns structure and texture without significant distinction. Besides, people resort to experience for creating the layout, but the external prior is also lacking in SinGAN, which makes it difficult to generate reasonable semantics or structure. These reasons lead to that the generative model learned from the image is inexplicable.

In this paper, our main contributions are: we propose a hierarchical framework for constructing an explainable single image generative model inspired by the painting process. We design ExSinGAN, which is learned from both the internal patches and the external prior of the given image. ExSinGAN is exactly explainable because it simulates the painting process through three cascaded GANs. Firstly, the structural GAN is devoted to synthesizing coarse but reasonable layout, then the semantic GAN is dedicated to adding semantic details to the coarse layout, finally, the texture GAN aims to replenish fine details. The latest GAN inversion technique [Pan *et al.*, 2020] is used for modeling structural prior, which we sample from to obtain training data. In addition, a new rescaling method is proposed for speeding up training. Figure 1 presents some syntheses of ExSinGAN, showing that our model can keep the structure of the input very well.

This paper is structured as follows: In section 2, we review recent works relevant to ours and analyze the advantages and shortcomings of existing methods. In section 3, we introduce our hierarchical framework to model the conditional distribution of a given image. In section 4 we introduce ExSinGAN in details. In section 5 we introduce important details in training ExSinGAN. In section 6 we show that, without any bells and whistles, our solid work takes a distinct improvement in synthesis, and possesses a competitive generalization ability for image manipulation tasks compared with prior works.

2 Related Work

Internal Learning Generative Model. [Shocher *et al.*, 2019] designed the first internal learning GANs called In-GAN to learn the internal distribution of image patches. In-GAN is a conditional GAN that requires the pre-defined geometric transformation to generate variety of images. Different from that, [Shaham *et al.*, 2019] were the first to propose an unconditional single image generative model called SinGAN, which contains a pyramid of fully convolutional GANs, and
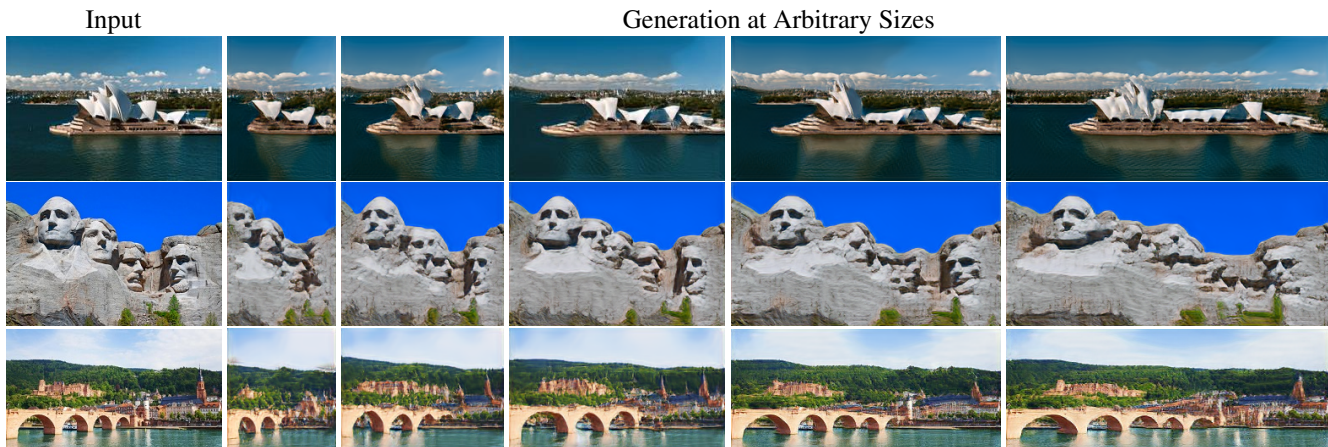
Input Generation at Arbitrary Sizes

Figure 1: Some syntheses of ExSinGAN. Since ExSinGAN has a specific module to learn the structural information, its syntheses have reasonable layouts similar to the inputs.

each stage of generators uses residual block [He *et al.*, 2016] for adding details. [Hinz *et al.*, 2021] proposed ConSinGAN for improving SinGAN by reducing model capacity, training several stages in parallel and propagating feature maps to the next stage. These improvements make ConSinGAN trained faster and perform competitively, nevertheless lose the flexibility like SinGAN, *e.g.*, it needs to design new training strategies when generalizing to other tasks. Recently, [Chen *et al.*, 2021] propose MOGAN to synthesize the ROI region and the rest region of the image respectively, then merge them together. One-Shot GAN [Sushko *et al.*, 2021] contains the multiple discriminators to learn the low level features, content and layout of the given image. [Granot *et al.*, 2021] borrow the idea from SinGAN and the classical PatchMatch [Barnes *et al.*, 2009] method to construct a novel non-training model called GPNN that generates a new image quickly. Because of only acquiring internal patches of the image, the internal learning methods are limited not only in terms of semantics, but also structure compared with methods trained on large scale dataset.

Generative Priors and Model Inversion. Different from the internal learning method, the model inversion method can utilize the pre-trained deep learning models as the external generative priors to conduct image synthesis. The mostly used pre-trained models includes the classifiers [Wang *et al.*, 2021] and GANs [Xia *et al.*, 2021], in this paper we focus the most popular way GAN inversion. GAN inversion aims at finding a code in the latent space of a pre-trained GAN that best reconstructs the given image. Once the optimal latent code is found, it can synthesize new images through manipulating the latent code. Recently, some works [Bau *et al.*, 2020; Pan *et al.*, 2020] have made progress in GAN inversion by joint optimization, which not only optimizes the latent code but also fine-tunes the parameters of the generator simultaneously. The DGP [Pan *et al.*, 2020] fine-tunes the generator of BigGAN [Brock *et al.*, 2019] pre-trained on *ImageNet* [Deng *et al.*, 2009] in a progressive manner, giving rise to more precise and faithful reconstruction for real images. Ideally, at the end of the process, DGP can find the optimal latent code

and obtain a degraded generator solely modeling the distribution of the given image. However, a critical issue is that the BigGAN is a conditional GAN that requires the class label. Though recently [Huh *et al.*, 2020] proposed an algorithm trying to solve the mixed optimization problem, the limited category of *ImageNet* means that the given image, *e.g.*, texture image or art painting, may not come from the pre-trained BigGAN at all. Besides, inverting the image of arbitrary size or resolution is also an intractable problem. Nonetheless, the fact that BigGAN has learned from lots of natural images indicates the degraded generator still has a better grasp of the structure of the image. If the internal learning method can benefit from it, it is promising to build a better single image generative model.

3 Hierarchical Framework for Generation

Abstractly, supposed that all images belong to the idea manifold $\mathcal{M}$, and each image $x = (x_{str}, x_{sem}, x_{tex})$, where $x_{str}, x_{sem}, x_{tex}$ lie on the submanifold $\mathcal{M}_{str}, \mathcal{M}_{sem}, \mathcal{M}_{tex}$, which represent the spaces of structural (or layout), semantic and texture information of the images respectively. This information can be defined by different formats, *e.g.*, the traditional descriptors, features learned by neural networks or just pixels. We name above representation of image as *triplet representation*. Apart from intuition, the representation does make practical sense, actually, it is based on the *three levels of content retrieval* proposed by [Eakins, 1996], which has played an important role in content-based image retrieval [Liu *et al.*, 2007]. The *three levels* respectively are: *primitive* features describing color or texture, *logical* features representing objects, and *abstract* attributes depicting the scenes, which is similar in meaning to our *triplet representation*.

Given an image $\hat{x}$, our goal is to model the conditional distribution $p(x|\hat{x})$. Having the *triplet representation*, then applying the probability multiplication formula to it, we can get the significant equation

$$p(x|\hat{x}) = p(x_{str}|\hat{x}) \cdot p(x_{sem}|x_{str}, \hat{x}) \\ \cdot p(x_{tex}|x_{str}, x_{sem}, \hat{x}), \quad (1)$$
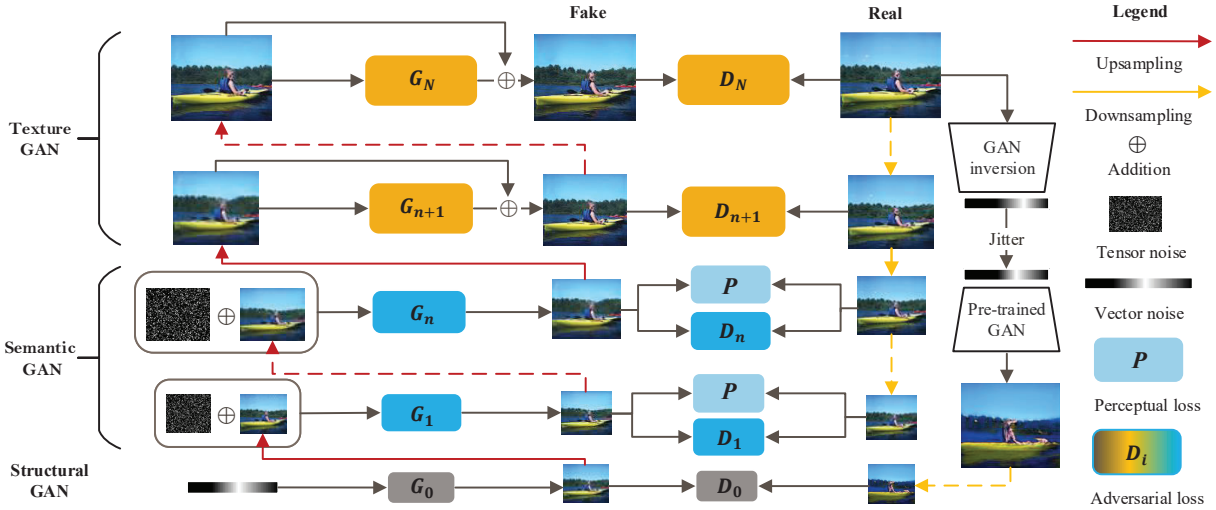
Figure 2: The architecture of ExSinGAN, which is composed of three cascaded GANs, the structural GAN for generating the coarse layout, semantic GAN for constraining the semantics of synthesis, the texture GAN for making the synthesis exquisite. Except for structural GAN, both semantic GAN and texture GAN are multi-stage. The GAN inversion is used for generating samples to train the structural GAN.

which breaks down $p(x|\hat{x})$ into three cascaded components meaningfully. The equation (1) has clearly expressed our hierarchical framework, namely obtaining $p(x|\hat{x})$ via modeling three new conditional distributions successively. The first term $p(x_{str}|\hat{x})$ is the *p.d.f* of structure, meeting that the synthesis with plausible layout should be sampled from more likely, and vice versa. The second term $p(x_{sem}|x_{str}, \hat{x})$ is the *p.d.f* of semantic information, in a practical sense it can be approximated by Gaussian or Dirac distribution since x_{sem} is determined by $\hat{x}_{sem}$ to a large extent. The last term $p(x_{tex}|x_{str}, x_{sem}, \hat{x})$ is the *p.d.f* of texture while we have known x_{str}, x_{sem}. Hence this term just requires that image x should have reasonable texture details based on existing conditions. Note that this framework is exactly consistent with the painting process we have described in section 1.

4 Methodology

In this section, we introduce ExSinGAN, which is intended to approximate $p(x|\hat{x})$ implicitly. Figure 2 shows the overview of ExSinGAN, where the network comprises three cascaded GANs, respectively the structural GAN, semantic GAN and texture GAN aiming to model $p(x_{str}|\hat{x})$, $p(x_{sem}|x_{str}, \hat{x})$ and $p(x_{tex}|x_{str}, x_{sem}, \hat{x})$ successively. Based on equation (1), the generative model learned by ExSinGAN is hierarchical and explainable, which is exactly different from SinGAN.

Structural GAN. In order to learn the structure, we need to give an explicit definition of the structural information of an image x. According to the multiresolution analysis, downscaling the image weakens the semantics and texture but keeps the layout farthest. That means defining x_{str} as x^0, where $\hat{x}^0$ is the subsampled version of x at proper size, indeed makes sense though we don't know the M_{str} at all. We denote the structural generator and discriminator as G_0 and D_0 respectively. Because the pre-trained BigGAN grasps the layout of the image well, the subsampled syntheses from DGP

of $\hat{x}$ that can be viewed as samples from $p(x_{str}|\hat{x})$, represents both the real images and structural information for training D_0, and the x^0 generated by G_0 represents both the fake image and structural information for deceiving D_0. To save training time, we set the size of x^0 to 32×32, so that G_0 is the simplest generator composed of one fully connected layer and three transposed convolutional layers, and D_0 is symmetrical containing three convolutional layers and one fully connected layer. We use WGAN-GP loss [Gulrajani *et al.*, 2017]

$$\min_{G_0} \max_{D_0} \mathcal{L}_{adv}(G_0, D_0) \qquad (2)$$

as the adversarial loss of structural GAN to keep training stable. Once the structural GAN is trained, $p(x_{str}|\hat{x})$ has been approximated by G_0 implicitly.
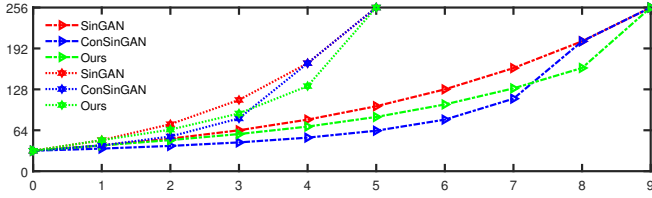
Semantic GAN. Supposed that $p(x_{sem}|x_{str}, \hat{x})$ is Gaussian and using pre-trained CNN for extracting semantic information, maximizing the probability is equivalent to minimizing the perceptual loss $\mathcal{L}_p(x, \hat{x}) = \|\phi(x) - \phi(\hat{x})\|$ proposed by [Johnson *et al.*, 2016] , where $\phi(x)$ represents the feature maps extracted from x by pre-trained CNN. To extract semantic information, the size of sample should be larger than that of x_{str}, which means that semantic GAN needs to enlarge x^0 with semantic constraint. Existing research [Sajjadi *et al.*, 2017; Zhou *et al.*, 2018] proves that the perceptual loss is helpful for better visual quality on image restoration task, nevertheless produces artifacts into the structures and causes color distortions. To avoid these artifacts, we use a pyramid of GANs with n stages for enlarging x_0 gradually,

$$x^s = G_s(x^{s-1}_\uparrow + z^s), \ s = 1, \dots, n. \qquad (3)$$

The subscript "$\uparrow$" means upsampling, and z^s is the noise at stage s. Both G_s and D_s comprise five convolutional layers. We do not use residual learning in semantic GAN since it will cause serious artifacts in practice (Figure 3e). The reconstruction loss $\mathcal{L}_{rec}(G_s) = \|G_s(\hat{x}^{s-1}_\uparrow) - \hat{x}^s\|^2$ is used

| (a) Original | (b) Sin.B. | (c) Sin.C. | (d) Ex.C. | (e) Ex.R. |

(f) Comparison of different rescaling methods

Figure 3: Given that $N = 9$, (a) original image. (b) SinGAN with its basic rescaling method. (c) SinGAN with the rescaling method of ConSinGAN. (d) ExSinGAN with the rescaling method of ConSin-GAN. (e) ExSinGAN using residual learning in semantic GAN. (f) comparison of different rescaling methods when $N = 5$ and 9, the horizontal and vertical axes respectively represent stage and pixel.

for ensuring $p(\hat{x}_{sem}|\hat{x}_{str}, \hat{x})$ does not vanish. We denote $\mathcal{L}_p(G_s(x_\uparrow^{s-1} + z^s), \hat{x}^s)$ as $\mathcal{L}_p(G_s)$, the total training loss is

$$\min_{G_s} \max_{D_s} \mathcal{L}_{adv}(G_s, D_s) + \alpha_1 \mathcal{L}_{rec}(G_s) + \lambda \mathcal{L}_p(G_s). \quad (4)$$

For arbitrary x^0 from G_0, the output x^n has similar layout to x^0 and close semantics to $\hat{x}$, which means $p(x_{sem}|x_{str}, \hat{x})$ has been expressed by semantic GAN implicitly.

Texture GAN. Though $p(x_{tex}|x_{str}, x_{sem}, \hat{x})$ seems hard to model, sampling from the distribution is essentially a reference-based super-resolution task that aims to restore x from x^n under the assumption that x has been determined by x_{str}, x_{sem} and $\hat{x}$. The top stages of SinGAN are suitable for this task, because the multi-stage architecture with the residual block that is widely used in super-resolution models [Kim *et al.*, 2016] can learn the texture furthest. Therefore, we set the architecture of texture GAN as the same as SinGAN,

$$x^s = G_s(x_\uparrow^{s-1}) + x_\uparrow^{s-1}, \ s = n + 1, \dots, N. \quad (5)$$

The training loss for each stage of the texture GAN is ,

$$\min_{G_s} \max_{D_s} \mathcal{L}_{adv}(G_s, D_s) + \alpha_2 \mathcal{L}_{rec}(G_s). \quad (6)$$

The noise z is not used due to the above-mentioned assumption. Thus, we have approximated $p(x|\hat{x})$ by these GANs.

5 Implementation

Rescaling method. The rescaling method influences both quality of synthesis and training time obviously. Supposed the height H of $\hat{x}$ is longer than the width W, we first prepro-cess $\hat{x}$ into $\hat{x}^N$ so that the longer side H_N is no more than 256. SinGAN takes the basic rescaling method $H_s = H_N \times r^{N-s}$, where r is scalar factor. ConSinGAN designs a complicated formula paying more attention to the layout, which performs better when N is small but will cause serious artifacts if N is large (Figure 3c). Though ExSinGAN is robust to it (Figure

3d), to save training time, we design a new rescaling method by analogous Taylor approximation

$$H_s = H_0 \times (1 + st + \frac{s(s-1)(s-2)}{k}t^3), \ s = 0, \dots, N. \quad (7)$$

In above equation, $t = \frac{1}{r} - 1$, k is adjustable. We set $k = 2$, the shorter side $W_0 = 32$ by default, r is determined by N. Figure 3f shows that the slope of our method does not vanish at original point, and become larger in the end, which is better self-adaptive to the change of N. Note that x^0 needs to be reshaped from 32×32 to $H_0 \times W_0$ before upsampled.

GAN inversion. We have experimented that using 128×128 or 256×256 pre-trained BigGAN for inversion almost had no difference to the results, hence we adopt 128×128 BigGAN in the following manipulation for efficiency. The process of generating training data is as follows: Firstly, we invert the given image into latent code by DGP with a random class label, then we jitter the code by Gaussian noise with mean 0, and standard deviations $\{0.1, 0.2, 0.3, 0.4, 0.5\}$. We sample 100 times at each level and get 500 training data in total. We use the last five layers of the discriminator for fine-tuning the generator, making DGP more stable.

Perceptual loss. Existing works used the convolutional lay-ers of pre-trained VGG-19 [Simonyan and Zisserman, 2015] for computing perceptual loss. We have tried the different convolutional layers of VGG-19 in advance and concluded that the combination of layers from '*relu*51' to '*relu*53' is the best choice for our model. We also attempted to use the last layer of the BigGAN discriminator for computing the percep-tual loss and found that it had a similar effect with VGG-19 (see the image at the upper right corner of Figure 6), declaring that the discriminator can extract strong semantic information like VGG-19. However, the discriminator has more enormous parameters compared with the convolutional layers of VGG-19 (87 million versus 20 million), hence we choose VGG-19 for computing perceptual loss for faster training.

Miscellaneous. We did our experiments with NVIDIA GeForce RTX 2080Ti. To take trade of training time and per-formance, we set $N = 6$, $n = 3$, $\lambda = 0.1$, $\alpha_1, \alpha_2 = 10$. For structural GAN, we set training epochs to 10k, learning rate to 10^{-4} for both G_0 and D_0, batch size to 32. Once the training process is finished, structural GAN can be reused for arbitrary models with different n and N. For the semantic and texture GAN, we set training epochs to 2k, learning rate to 5×10^{-4} for G_i and D_i, $i = 1, \dots, N$. Batch Normalization [Ioffe and Szegedy, 2015] is used in each stage of ExSinGAN.

6 Experimental Results

In this section, we compare ExSinGAN (seven stages) with DGP[1] (random class label), SinGAN[2] (about ten stages) and ConSinGAN[3] (six stages) on image synthesis, editing, har-monization and paint-to-image tasks. All these methods are set to their official setups. Training ExSinGAN with our

---

[1] https://github.com/XingangPan/deep-generative-prior
[2] https://github.com/tamarott/SinGAN
[3] https://github.com/tohinz/ConSinGAN

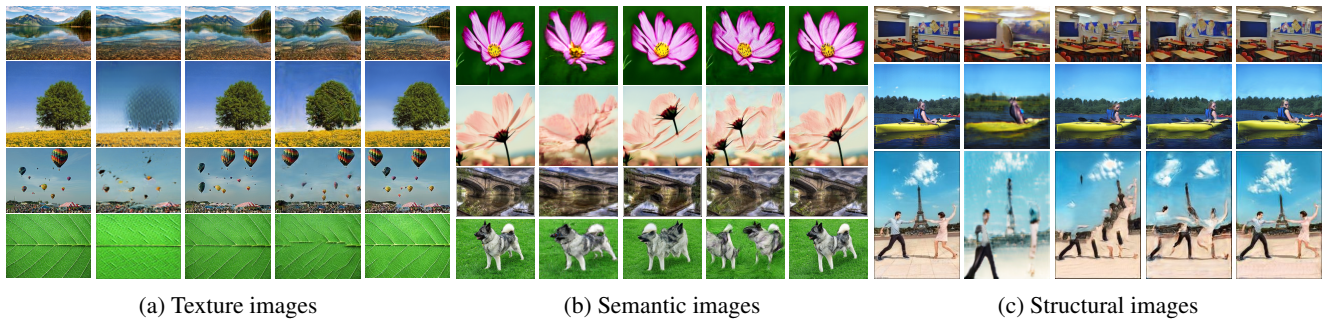| (a) Texture images | (b) Semantic images | (c) Structural images |

Figure 4: Comparison of DGP, SinGAN, ConSinGAN, ExSinGAN on image synthesis. For each part, there are five columns, from left to right respectively are original, DGP, best syntheses of SinGAN, best syntheses of ConSinGAN, random syntheses of ExSinGAN.

Original	SinGAN	ConSinGAN	ExSinGAN	ExSinGAN
0.00 / 0.00	0.18 / 0.53	0.34 / 0.51	0.40 / 0.14	0.86 / 0.39

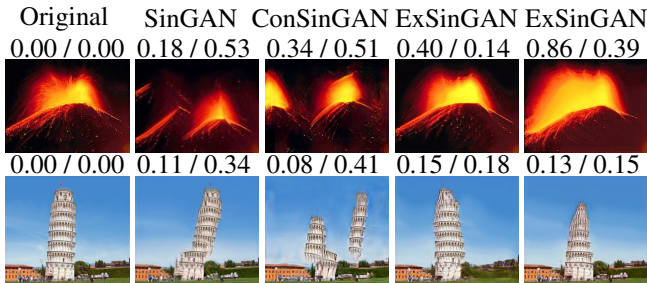| 0.00 / 0.00 | 0.11 / 0.34 | 0.08 / 0.41 | 0.15 / 0.18 | 0.13 / 0.15 |

Figure 5: Some syntheses of *Places50*. The second row shows their *SIFID* and *LPIPS*.

rescaling method costs about 45 min, saving about 20 min compared with using other rescaling methods. Training Sin-GAN and ConSinGAN cost 80 min and 20 min respectively. The overall comparison is provided in the Supplementary Materials.

6.1 Image Synthesis

We conduct experiments on various types of images for comprehensive comparison, including texture image with rich texture but the simple structure, semantic image containing a single complicated object in the scene, and structural image comprising the complex scene and several objects.

Texture images. Since people have a high tolerance for structural changes in texture pictures, this task primarily compares the ability to synthesize texture. See Figure 4a, the syntheses of DGP have unpromising texture, but ExSinGAN can obtain exquisite results rivaling SinGAN by revising these unsatisfactory images. Note that the syntheses of ConSinGAN have artifacts and coarse texture (the balloons and tree), and this phenomenon persists when we increase its stages.

Semantic images. See Figure 4b, objects in these images have strong semantic information, hence free deformation in texture or structure is no longer permitted. SinGAN and Con-SinGAN performed passably on the first flower, confused with the relation of petals, and ignoring the flower stalk. However, they are completely frustrated by the second flower, although the structures of the two flowers have only a slight difference. In fact, through experiments we found that Sin-GAN and particularly ConSinGAN were sensitive to the color

change. Note that the color of the first flower is distinct from the background color, therefore, they can perceive the existence of the petals rather than the stalk. Similarly, they can perceive the existence of the stalk rather than the petals for the second flower. ExSinGAN not only successfully synthesized the petals but also generated the stalk beneath the petals for the two flowers. The bridge and hound images show that SinGAN and ConSinGAN could not capture the structure yet, but ExSinGAN is stable enough to generate delicate syntheses with both fine details and reasonable structures benefiting from structural GAN and semantic constraint.

Structural images. See Figure 4c, the first image contains many objects with regular shapes, while the syntheses of Sin-GAN and ConSinGAN are disorganized and messy. The second and third rows show they do not take into account the relationships between the human and boat, or the dancing people and tower. Despite DGP performs badly in texture, ExSinGAN just properly utilizes its merit of generating reasonable layouts, making reasonable variations in images.

Quantitative evaluation. Evaluating the single image generation method quantitatively is really an open and difficult problem. From the perspective of evaluation principle, we believe that a complete evaluation should contain the measurement of perception, such as whether the image and its syntheses come from the same category, and the measurement of the diversity. Moreover, the perceptual similarity takes more important role than the diversity, due to we observe the generators are more likely to synthesize meaningless images, *e.g.*, the elkhound in Fig. 4b. Unlike that the large scale dataset usually has a relatively valid statistical metric, *e.g.*, *FID*, single image task lacks the effective statistical metric since the estimations of statistical indicators, *e.g.*, mean and variation, are highly biased. SinGAN proposed *SIFID* to compare the distribution of the original image with that of its syntheses using the feature extracted by the pre-trained Inception network [Szegedy *et al.*, 2015]. However, we observe that the estimation is deviated from the truth sometimes. In Fig. 5, we compare the images with their syntheses by the *SIFID* metric. Although the fourth and fifth column images are similar to the first column images in vision, they are of higher *SIFID* than the second and third column images. Therefore, we adopt the *LPIPS* [Zhang *et al.*, 2018] that calibrated the AlexNet [Krizhevsky *et al.*, 2017]

Model	Places50			LSUN50			ImageNet50			Mean		
	SIFID↓	LPIS↓	SSIM↓	SIFID↓	LPIS↓	SSIM↓	SIFID↓	LPIS↓	SSIM↓	SIFID↓	LPIS↓	SSIM↓
ConSinGAN	**0.06**	0.24	0.25	0.11	0.32	0.26	0.56	0.39	0.23	0.24	0.32	0.25
SinGAN	0.09	0.25	0.37	0.23	0.33	0.33	0.60	0.33	0.34	0.31	0.30	0.35
ExSinGAN	0.09	**0.23**	0.34	**0.11**	**0.25**	0.35	**0.45**	**0.24**	0.34	**0.22**	**0.24**	0.34
Te.1 Se.3 Te.3	0.23	0.42	**0.20**	0.28	0.52	**0.19**	0.56	0.51	**0.20**	0.36	0.48	**0.20**
St.1 Se.0 Te.6	0.17	0.24	0.32	0.17	0.28	0.31	0.5	0.29	0.27	0.28	0.27	0.30
St.1 Se.1 Te.5	0.15	0.24	0.34	0.15	0.26	0.34	0.54	0.25	0.34	0.28	0.25	0.34
St.1 Se.3 Te.3	0.09	0.23	0.34	0.11	0.25	0.35	0.45	0.24	0.34	0.22	0.24	0.34
St.1 Se.6 Te.0	0.11	0.35	0.35	0.11	0.25	0.35	0.50	0.25	0.34	0.24	0.28	0.35

Table 1: Evaluations of *SIFID*, *LPIPS*. and *SSIM* on the *Places50*, *LSUN50*, and *ImageNet50*. The St., Se. and Te. are the abbreviations of Structural GAN, Semantic GAN and Texture GAN. The numbers behind them are their stages. Note that ExSinGAN is identical with St.1 Se.3 Te.3. *Mean* is the average results on the three datasets
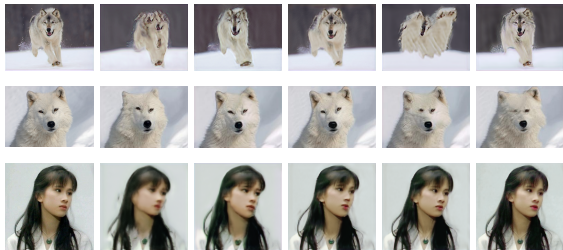

Figure 6: Examples for ablation study. From left to right, first row: original, SinGAN, structural GAN with texture GAN, ExSinGAN, semantic GAN with texture GAN, using the discriminator of Big-GAN for computing perceptual loss. Second row: original, and ExSinGAN with increasing n from 1 to 5. Third row: original, and ExSinGAN with increasing N from 5 to 9.

using human perceptual judgments as the perceptual metric for this task. Note that prior works [Choi *et al.*, 2020] have used the higher *LPIPS* to show the diversity between origin and syntheses, in those works the origin and syntheses locate in different domains. However, the internal learning syntheses and origin should in the same domain. Therefore, the smaller the LIPIS, the better the quality of the syntheses. Fig. 5 shows that *LPIPS* is more faithful than *SIFID*. We use *SIFID* and *LPIPS* as the metrics for the perceptual similarity, and *SSIM* for the diversity. We evaluate SinGAN, ConSin-GAN, and ExSinGAN on three datasets, *Places50* proposed by SinGAN consisting of 50 images from the *Places* dataset [Zhou *et al.*, 2014], *LSUN50* proposed by ConSinGAN consisting 50 images from the *LSUN* dataset [Yu *et al.*, 2015]. The two datasets mainly contain scenes rather than objects that are more sensitive to deformation, hence we construct the *ImageNet50* by sampling 50 images containing objects of different sizes from the validation set of *ImageNet*. In Table 1, ExSinGAN achieves the best *LPIPS* in all datasets, the best average *SIFID* and *LPIPS*, and holds the similar *SSIM* like SinGAN, proving that the hierarchical and explainable design of ExSinGAN is highly effective to learn a pretty generative model.

6.2 Ablation Study

In this subsection, we conduct the ablation study on ExSin-GAN to verify our improvements in SinGAN effectiveness. Our baseline is the SinGAN (namely texture GAN) of 7 stages and training setups are the same with section 5.

Structural GAN. See the first row of Figure 6, the image generated by baseline is a failure. For proving the significance of structural GAN, we just replace the first stage of SinGAN with structural GAN, the *SIFID* and *LPIPS* decrease overtly (St.1 Se.0 Te.6 in Table 1), and the synthesis (the third image) has an overtly clearer appearance than before. We point that by increasing the training epochs from 10k to 20k, the syntheses are of better quality and lower failure rate, nevertheless the training process will cost an extra 10 min than before. The increase of model capacity has these effects as well.

Semantic GAN. Now we combine the Structural GAN with Semantic GAN to show their effects further. See the first row of Figure 6, the fourth image (ExSinGAN) shows that the skin of the wolf is smoother and tidier than the previous one (St.1 Se.0 Te.6). Then we withdraw the structural GAN (Te.1 Se.3 Te.3), the result (the fifth image) shows that all syntheses are failures. It means that the structural GAN is necessary for the successful generation, and the semantic GAN is a helper to make the synthesis more realistic and meaningful. They promote and affect each other. In Table 1, the quantitative results shows that only Semantic GAN has the negative effect to baseline (bad initial estimation), but positive effect to structural GAN (good initial estimation).

Number of stages. The number of stages also greatly influences the results and the cost of time. For ExSinGAN, there are two hyper-parameters N and n should be considered. We firstly fix $N = 6$ and increase n from 1 to 5, the second row of Fig. 6 shows that the semantics of syntheses is closer to the original image as n is increased. However, since the high-level feature maps also contain information for image restoration, once the size of the feature map is too large, the perceptual loss is almost equivalent to per-pixel loss, which is inconsistent with the purpose of semantic constraint and adds artifacts to the syntheses. The quantitative results (St.1 Se.0 Te.6, St.1 Se.1 Te.6, ExSinGAN, and St.1 Se.6 Te.0)

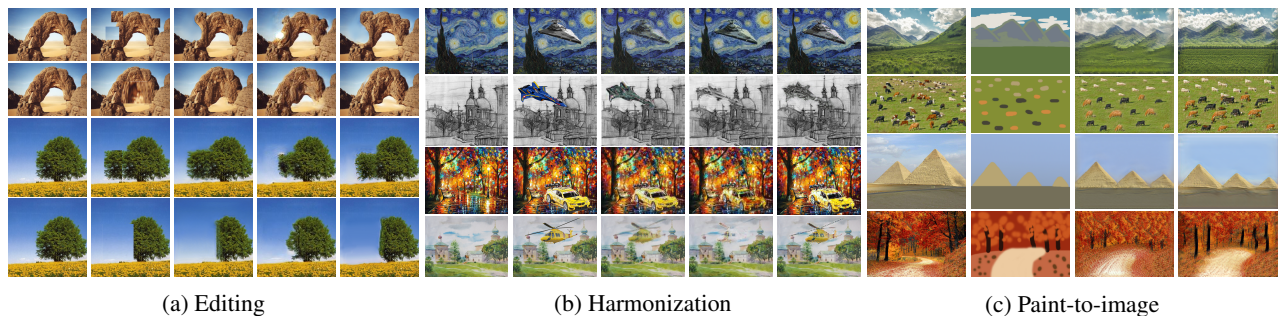| (a) Editing | (b) Harmonization | (c) Paint-to-image |

Figure 7: Generalization study. For editing and harmonization, the five columns respectively are original, naive, SinGAN, ConSinGAN, ExSinGAN. For paint-to-image, the four columns are original, painting, SinGAN, ExSinGAN.

shows that *SIFID* and *LPIPS* firstly decrease and then increase, proving that $n = 3$ is the best choice. We do not conduct quantitative study about N since there has been similar research in [Shaham *et al.*, 2019] and [Hinz *et al.*, 2021]. We just show an example in Fig. 6, when increasing N from 5 to 9, the stage of semantic GAN is increased but constrained by the size of the output of no more than 70 pixels. The third row of Figure 6 shows that we can get higher quality syntheses with N increased, but smaller changes of structure and more time consuming (a double-time when $N = 9$).

6.3 Generalization Study

In this subsection, we show that ExSinGAN also has a powerful generalization ability (Figure 7). We use pre-trained models of synthesis without any fine-tune for editing, harmonization and paint-to-image, all of which need sample from $p(x_{tex}, x_{sem}|\hat{x}, x_{str})$.

Editing. This task aims to produce a seamless composite in which image regions have been copied and pasted in other locations. For ExSinGAN, we inject a subsampled version of the naive image into stage one as x_{str}, then combine the synthesis with the original image at the edited regions. Figure 7a shows some examples of three methods, for the stone images, ExSinGAN can do better in generating a more realistic texture than the other two methods. For the tree images, ExSinGAN can keep the structures of naive images well, which means ExSinGAN is more controllable. ConSinGAN failed to merge the background in this task.

Harmonization. Image harmonization aims to realistically blend a pasted object with a background image. For SinGAN and ExSinGAN, the harmonization process is identical to the editing process. The results in Figure 7b show that our work still gets better results compared with SinGAN. ConSinGAN can get better results sometimes since it fine-tunes the models by the naive image.

Paint-to-image. See Figure 7c, this task aims to transfer a paint into a photo-realistic image. Because ConSinGAN does not support this task, we just compare ExSinGAN with SinGAN. For SinGAN, this is done by subsampling the paint and feeding it into one of the coarse scales. For ExSinGAN, we just feed the subsampled painting into stage one. From these images, we know that ExSinGAN is sensitive to the struc-

ture of paint (the road under trees, the grass near the mountains), and the texture and style are more realistic (the cows). For the pyramids, the synthesis of ExSinGAN is more three-dimensional and context-based (the clouds around pyramids). In conclusion, ExSinGAN can do this task better than SinGAN with fewer stages and time consumption.

7 Conclusion

We introduced ExSinGAN, an explainable single image generative model based on the hierarchical framework of generation. We demonstrated it has better abilities in synthesis and generalization compared with prior works. Though many improvements can be made on ExSinGAN, *e.g.*, the concurrent training as ConSinGAN did and building more complex networks, we think the most meaningful thing is integrating more valid external priors into ExSinGAN to make it more intelligent, which we will explore further in our future works.

References

[Barnes *et al.*, 2009] Connelly Barnes, E. Shechtman, A. Finkelstein, and Dan B. Goldman. Patchmatch: a randomized correspondence algorithm for structural image editing. In *SIGGRAPH 2009*, 2009.

[Bau *et al.*, 2020] David Bau, Hendrik Strobelt, William Peebles, Bolei Zhou, Jun-Yan Zhu, Antonio Torralba, et al. Semantic photo manipulation with a generative image prior. *arXiv preprint arXiv:2005.07727*, 2020.

[Brock *et al.*, 2019] Andrew Brock, Jeff Donahue, and Karen Simonyan. Large scale GAN training for high fidelity natural image synthesis. In *International Conference on Learning Representations*, 2019.

[Chen *et al.*, 2021] J. Chen, Qihui Xu, Qi Kang, and M. Zhou. Mogan: Morphologic-structure-aware generative learning from a single image. *ArXiv*, abs/2103.02997, 2021.

[Choi *et al.*, 2020] Yunjey Choi, Youngjung Uh, J. Yoo, and Jung-Woo Ha. Stargan v2: Diverse image synthesis for multiple domains. *2020 IEEE/CVF Conference on Computer Vision and Pattern Recognition (CVPR)*, pages 8185–8194, 2020.

[Deng *et al.*, 2009] Jia Deng, Wei Dong, Richard Socher, Li-Jia Li, Kai Li, and Li Fei-Fei. Imagenet: A large-scale hierarchical image database. In *2009 IEEE conference on computer vision and pattern recognition*, pages 248–255. Ieee, 2009.

[Eakins, 1996] John P Eakins. Automatic image content retrieval-are we getting anywhere? In *Proceedings of Third International Conference on Electronic Library and Visual Information Research*, pages 123–135, 1996.

[Goodfellow *et al.*, 2014] Ian Goodfellow, Jean Pouget-Abadie, Mehdi Mirza, Bing Xu, David Warde-Farley, Sherjil Ozair, Aaron Courville, and Yoshua Bengio. Generative adversarial nets. In *Advances in neural information processing systems*, pages 2672–2680, 2014.

[Granot *et al.*, 2021] Niv Granot, Assaf Shocher, Ben Feinstein, S. Bagon, and M. Irani. Drop the gan: In defense of patches nearest neighbors as single image generative models. *ArXiv*, abs/2103.15545, 2021.

[Gulrajani *et al.*, 2017] Ishaan Gulrajani, Faruk Ahmed, Martin Arjovsky, Vincent Dumoulin, and Aaron C Courville. Improved training of wasserstein gans. In *Advances in neural information processing systems*, pages 5767–5777, 2017.

[He *et al.*, 2016] Kaiming He, Xiangyu Zhang, Shaoqing Ren, and Jian Sun. Deep residual learning for image recognition. In *Proceedings of the IEEE conference on computer vision and pattern recognition*, pages 770–778, 2016.

[Hinz *et al.*, 2021] Tobias Hinz, Matthew Fisher, Oliver Wang, and Stefan Wermter. Improved techniques for training single-image gans. In *Proceedings of the IEEE/CVF Winter Conference on Applications of Computer Vision*, pages 1300–1309, 2021.

[Huh *et al.*, 2020] Minyoung Huh, Richard Zhang, Jun-Yan Zhu, Sylvain Paris, and Aaron Hertzmann. Transforming and projecting images into class-conditional generative networks. *arXiv preprint arXiv:2005.01703*, 2020.

[Ioffe and Szegedy, 2015] Sergey Ioffe and Christian Szegedy. Batch normalization: Accelerating deep network training by reducing internal covariate shift. In *International Conference on Machine Learning*, pages 448–456, 2015.

[Johnson *et al.*, 2016] Justin Johnson, Alexandre Alahi, and Li Fei-Fei. Perceptual losses for real-time style transfer and super-resolution. In *European conference on computer vision*, pages 694–711. Springer, 2016.

[Kim *et al.*, 2016] Jiwon Kim, Jung Kwon Lee, and Kyoung Mu Lee. Accurate image super-resolution using very deep convolutional networks. In *Proceedings of the IEEE conference on computer vision and pattern recognition*, pages 1646–1654, 2016.

[Krizhevsky *et al.*, 2017] Alex Krizhevsky, Ilya Sutskever, and Geoffrey E Hinton. Imagenet classification with deep convolutional neural networks. *Communications of the ACM*, 60(6):84–90, 2017.

[Liu *et al.*, 2007] Y. Liu, Dengsheng Zhang, G. Lu, and W. Ma. A survey of content-based image retrieval with high-level semantics. *Pattern Recognit.*, 40:262–282, 2007.

[Pan *et al.*, 2020] Xingang Pan, Xiaohang Zhan, Bo Dai, Dahua Lin, Chen Change Loy, and Ping Luo. Exploiting deep generative prior for versatile image restoration and manipulation. *arXiv preprint arXiv:2003.13659*, 2020.

[Sajjadi *et al.*, 2017] Mehdi S. M. Sajjadi, B. Schölkopf, and M. Hirsch. Enhancenet: Single image super-resolution through automated texture synthesis. *2017 IEEE International Conference on Computer Vision (ICCV)*, pages 4501–4510, 2017.

[Shaham *et al.*, 2019] Tamar Rott Shaham, Tali Dekel, and T. Michaeli. Singan: Learning a generative model from a single natural image. *2019 IEEE/CVF International Conference on Computer Vision (ICCV)*, pages 4569–4579, 2019.

[Shocher *et al.*, 2019] Assaf Shocher, S. Bagon, Phillip Isola, and M. Irani. Ingan: Capturing and retargeting the "dna" of a natural image. *2019 IEEE/CVF International Conference on Computer Vision (ICCV)*, pages 4491–4500, 2019.

[Simonyan and Zisserman, 2015] K. Simonyan and Andrew Zisserman. Very deep convolutional networks for large-scale image recognition. *CoRR*, abs/1409.1556, 2015.

[Sushko *et al.*, 2021] V. Sushko, Juergen Gall, and A. Khoreva. One-shot gan: Learning to generate samples from single images and videos. *ArXiv*, abs/2103.13389, 2021.

[Szegedy *et al.*, 2015] Christian Szegedy, Wei Liu, Yangqing Jia, Pierre Sermanet, Scott Reed, Dragomir Anguelov, Dumitru Erhan, Vincent Vanhoucke, and Andrew Rabinovich. Going deeper with convolutions. In *Proceedings of the IEEE conference on computer vision and pattern recognition*, pages 1–9, 2015.

[Wang *et al.*, 2021] Pei Wang, Yijun Li, Krishna Kumar Singh, Jingwan Lu, and N. Vasconcelos. Imagine: Image synthesis by image-guided model inversion. *ArXiv*, abs/2104.05895, 2021.

[Xia *et al.*, 2021] Weihao Xia, Yulun Zhang, Yujiu Yang, Jing-Hao Xue, Bolei Zhou, and Ming-Hsuan Yang. Gan inversion: A survey. *arXiv preprint arXiv:2101.05278*, 2021.

[Yu *et al.*, 2015] Fisher Yu, Ari Seff, Yinda Zhang, Shuran Song, Thomas Funkhouser, and Jianxiong Xiao. Lsun: Construction of a large-scale image dataset using deep learning with humans in the loop. *arXiv preprint arXiv:1506.03365*, 2015.

[Zhang *et al.*, 2018] Richard Zhang, Phillip Isola, Alexei A Efros, Eli Shechtman, and Oliver Wang. The unreasonable effectiveness of deep features as a perceptual metric. In *Proceedings of the IEEE conference on computer vision and pattern recognition*, pages 586–595, 2018.

[Zhou *et al.*, 2014] Bolei Zhou, Agata Lapedriza, Jianxiong Xiao, Antonio Torralba, and Aude Oliva. Learning deep features for scene recognition using places database. *Advances in neural information processing systems*, 27:487–495, 2014.

[Zhou, *et al.*, 2018] Yang Zhou, Zhen Zhu, Xiang Bai, Dani Lischinski, Daniel Cohen-Or, and Hui Huang. Non-stationary texture synthesis by adversarial expansion. *ACM Transactions on Graphics (TOG)*, 37(4):1–13, 2018.